

IRAS04325+2402C: A VERY LOW MASS OBJECT WITH AN EDGE-ON DISK

ALEXANDER SCHOLZ¹, RAY JAYAWARDHANA², KENNETH WOOD¹, DAVID LAFRENIÈRE^{2,5}, KATHARINA SCHREYER³, RENÉ DOYON⁴

To appear in ApJL

ABSTRACT

IRAS04325+2402C is a low luminosity object located near a protostar in Taurus. We present new spatially-resolved mm observations, near-infrared spectroscopy, and Spitzer photometry that improve the constraints on the nature of this source. The object is clearly detected in our 1.3 mm interferometry map, allowing us to estimate the mass in a localized disk+envelope around it to be in the range of 0.001 to 0.01 M_{\odot} . Thus IRAS04325C is unlikely to accrete significantly more mass. The near-infrared spectrum cannot be explained with an extincted photosphere alone, but is consistent with a 0.03-0.1 M_{\odot} central source plus moderate veiling, seen in scattered light, confirming the edge-on nature of the disk. Based on K-band flux and spectral slope we conclude that a central object mass $\gtrsim 0.1 M_{\odot}$ is unlikely. Our comparison of the full spectral energy distribution, including new *Spitzer* photometry, with radiative transfer models confirms the high inclination of the disk ($\gtrsim 80^{\circ}$), the very low mass of the central source, and the small amount of circumstellar material. IRAS04325C is one of the lowest mass objects with a resolved edge-on disk known to date, possibly a young brown dwarf, and a likely wide companion to a more massive star. With these combined properties, it represents a unique case to study the formation and early evolution of very low mass objects.

Subject headings: stars: circumstellar matter, formation, low-mass, brown dwarfs – planetary systems

1. INTRODUCTION

The origin of brown dwarfs has been one of the most intensely debated subjects in cool stars research over the past decade. As of today, there is no consensus on the dominant mechanisms that determine the low-mass end of the stellar initial mass function. Recent modeling has provided predictions for observable properties in the very low mass (VLM) regime, which in principle would permit distinguishing between the proposed scenarios. In practice, however, it has turned out to be challenging to place firm limits on the formation theory for VLM sources (see reviews by Whitworth et al. 2007; Luhman et al. 2007b).

Of particular relevance for evaluating formation scenarios are the global properties of disks and envelopes. The combination of high-resolution imaging and analysis of the spectral energy distribution (SED) in the infrared/mm regime is generally acknowledged as the optimum source of information for disk/envelope parameters of young stellar sources. As of today, constraints on radii and masses of brown dwarf disks are sparse: Recent deep mm observations provided first limits on disk masses ($< 0.001 - 0.003 M_{\odot}$) and outer radii (10-100 AU; Scholz et al. 2006; Klein et al. 2003). Only one substellar disk has been resolved with high-resolution

imaging (Luhman et al. 2007a), with a derived radius of 20-40 AU.

In this context, the young source IRAS04325+2402C (hereafter: IRAS04325C) in the Taurus star forming complex may be of particular interest. HST/NICMOS images of the Class I source IRAS04325+2402 (Kenyon & Hartmann 1995), also known as L1535 IRS, revealed IRAS04325C as a faint companion, at a separation of 8''1 (Hartmann et al. 1999)⁶. The object is resolved 'into a double-lobed emission separated by a dark lane' (Hartmann et al. 1999), resembling the images of edge-on T Tauri disks. Models including an edge-on disk and an envelope are able to reproduce the appearance of the images. From the near-infrared (NIR) photometry, the mass of this possible Class I object was estimated to be between 0.02 and 0.06 M_{\odot} , with an upper limit of 0.25 M_{\odot} . Based on statistical arguments, Duchêne et al. (2004) find that the system is likely to be a physically bound binary (probability 98%).

Thus, IRAS04325C is a potential benchmark object to study substellar formation. In this Letter, we present new millimeter interferometry and NIR spectroscopy as well as an analysis of the resolved SED for this source, including new *Spitzer* photometry, with the aim of improving the constraints on the properties of the system, particularly the mass of the central object and the disk+envelope.

2. NEW CONSTRAINTS FROM RESOLVED OBSERVATIONS

2.1. Millimeter interferometry

Using the IRAM Plateau de Bure Interferometer (Guilloteau et al. 1992), we obtained a 1.3 mm (226.50 GHz) continuum map centered on IRAS04325C, ob-

⁶ Note that the primary itself is likely to be a subarcsecond binary, see Hartmann et al. (1999)

Electronic address: as110@st-andrews.ac.uk

¹ SUPA, School of Physics & Astronomy, University of St. Andrews, North Haugh, St. Andrews, KY16 9SS, United Kingdom

² Department of Astronomy & Astrophysics, University of Toronto, 50 St. George Street, Toronto, ON M5S 3H4, Canada

³ Astrophysikalisches Institut und Universitäts-Sternwarte Jena, Schillergässchen 2-3, D-07745 Jena, Germany

⁴ Département de Physique and Observatoire du Mont Mégantic, Université de Montréal, C.P. 6128, Succursale Centre-Ville, Montréal, QC H3C 3J7, Canada

⁵ Visiting Astronomer at the Infrared Telescope Facility, which is operated by the University of Hawaii under Cooperative Agreement no. NNX08AE38A with the National Aeronautics and Space Administration, Science Mission Directorate, Planetary Astronomy Program.

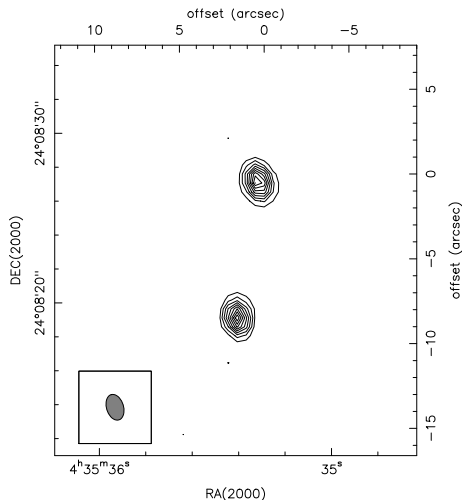


FIG. 1.— Interferometry map at 1.3 mm wavelength, obtained with the IRAM Plateau de Bure Interferometer. The map is centered on our target IRAS04325C; the primary source is seen at (+2", -8"). The inset in the lower left corner shows the beam size. The contours are 10% to 90% of the peak value in steps of 10%.

served on 27 December 2007 (configuration C, rms 0.3 mJy/beam, HPBW 1.55" \times 1.0"). The final map of 128 \times 128 square pixels with 0".53 pixel size was produced by Fourier transforming the calibrated visibilities using natural weighting using the Grenoble Software environment GAG.

The 1.3 mm image (Fig. 1) shows two sources, which are identified with the primary (south) and companion (north) object in the HST images from Hartmann et al. (1999). We estimate fluxes of 10 ± 3 mJy for both sources by integrating the pixel intensities. The 1.3 mm flux is attributed to thermal emission from cold dust. Since the peaks in the map are strongly centered at the positions of the infrared sources, the emission most likely originates from the disk and the localized envelope with a diameter $\lesssim 300$ AU. Assuming that the dust is optically thin, we can obtain an estimate of the total dust mass M_{dust} from the mm flux S_ν :

$$M_{\text{dust}} = \frac{S_\nu D^2}{B_\nu(T_D) \kappa_\nu} \quad (1)$$

We assume a distance D of 148 pc for the Taurus star forming region (Loinard et al. 2007), a gas to dust ratio of 100, and a plausible range of values for dust temperature T_D (10–25 K) and dust opacity κ_ν (1–3 cm²g⁻¹ at 1.3 mm), as commonly suggested in the literature (see Scholz et al. 2006, and references therein). Using these parameters, we obtain a total mass (dust and gas) of 1–10 M_{Jup} and a most probable value of 3 M_{Jup} for each of the two sources. This value is comparable to the highest disk mass determined for a Class II brown dwarf in Taurus (Scholz et al. 2006).

Single-dish measurements centered on IRAS04325 are available in the literature and can be used to put limits on the mass of a possible common envelope surrounding both the primary and the secondary. Published fluxes are ~ 180 mJy at 850 μm (15" beam, Hogerheijde & Sandell 2000; Andrews & Williams 2005), 110 mJy at 1.3 mm (11", Motte & André 2001), < 9.2 mJy at 3 mm ($\sim 11"$, Ohashi et al. 1996). Using the same parameters as above and $\kappa_\nu \propto \lambda^{-\beta}$ with $\beta \sim 1.5$ (Natta et al. 2007) yields corresponding masses of 10–30 M_{Jup} of distributed dust

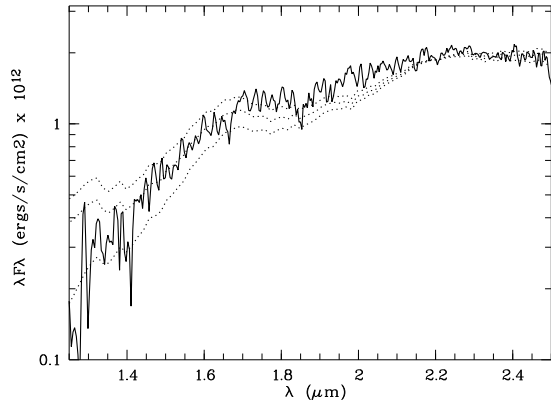


FIG. 2.— IRTF/SpeX spectrum for IRAS04325C (solid line) in comparison with models (dotted lines). All spectra are scaled to the K-band flux. The models assume $T_{\text{eff}} = 3000$ K and typical veiling. The three model spectra in the plot are calculated from three scattering models (MRN2, 12, 15 in Kenyon et al. 1993)

and gas in an area with diameter ~ 2000 AU around the primary IRAS source, including the companion. Fluxes integrated over larger areas (500 mJy for 60" diameter, Motte & André 2001) clearly indicate the presence of large-scale mm background in that area. Given that the primary in the system is probably more massive than the companion (see Sect. 4), IRAS04325C is unlikely to be the dominant center of accretion in that area. Thus, the total mass reservoir for IRAS04325C is 1–10 M_{Jup} in the localized disk/envelope plus presumably a small fraction of at most 30 M_{Jup} in a possible common envelope.

2.2. Near-infrared spectroscopy

We obtained a NIR (1–2.5 μm) low-resolution ($R \sim 100$) spectrum for IRAS04325C using SpeX at IRTF (Rayner et al. 2003). Reduction, background correction, and extraction was carried out using SpeXtools (Cushing et al. 2004). We corrected for instrument response and telluric features using a spectrum of the A0 star HD25175 observed immediately before the target. The final signal-to-noise ratio ranges from 15 in H- to 30 in K-band. Our spectrum rises steeply from J- to K-band and is lacking obvious photospheric features. The spectrum is shown in Fig. 2 (solid line) scaled to the published K-band flux (14.0–14.6 mag, Hartmann et al. 1999; Connelley et al. 2008). In the following, we will use the shape of the spectrum and the K-band flux to derive a constraint on the mass of the central source.

We compare the observed spectrum with models based on the photospheric templates STARDUSTY2000 and BD-DUSTY2000 (Allard et al. 2001). In a first attempt, we calculated a series of models assuming pure extinction, thus neglecting the edge-on nature (NIR extinction law from Mathis 1990). While it is possible to reproduce the slope of the spectrum using such models, the required combinations of T_{eff} and A_V imply photospheric K-band fluxes that are more than one order of magnitude larger than the observed value. Thus, pure extinction cannot account for the NIR SED, confirming that the object is seen in scattered light through an edge-on disk.

Thus, instead of extinction, we applied scattering models from Kenyon et al. (1993), which have been confirmed to fit the colours of embedded young stars in Taurus. For a range of scattering properties and edge-on geom-

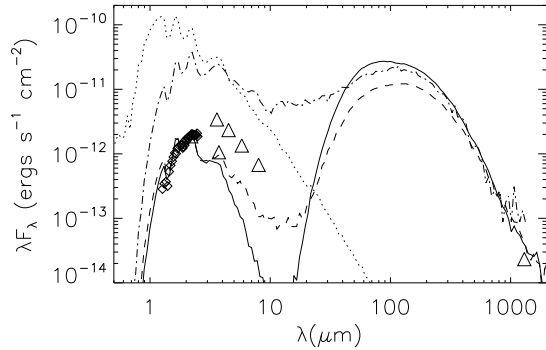


FIG. 3.— Spectral energy distribution for IRAS04325C in comparison with Monte Carlo radiative transfer models. Triangles and diamonds are the observed fluxes; Spitzer datapoints at $3.6\text{--}8\mu\text{m}$ are treated as upper limits. Solid line: model with ISM grains, dashed line: model with larger grains (see text), dash-dotted line: model with face-on geometry, dotted line: input photosphere. (All models include extinction of $A_V = 10$.)

etry, Kenyon et al. (1993) obtain 2.0–4.5 mag difference between observed and photospheric K-band flux, in line with the properties of many known edge-on disks. This implies for our target $M_K = 3.8 \dots 6.9$ mag. Comparison with the 1 Myr track by Baraffe et al. (1998) yields $T_{\text{eff}} = 2700 \dots 3200$ K and $M = 0.03 \dots 0.16 M_{\odot}$.

Photospheric spectra for this range of temperatures exhibit deep H_2O absorption features, which are not seen in our spectrum. The most likely reason for their absence is veiling, as frequently observed for young stellar sources (Greene & Lada 1996). We use the typical veiling for Class-II sources of $r_K = 1.76$ and $r_J = 0.97$ (Folha & Emerson 1999). If the K-band flux includes that amount of veiling, the upper limits for temperature and mass are reduced to $T_{\text{eff}} = 3000$ K and $M = 0.1 M_{\odot}$.

For both scattering and veiling, we fit the values for the photometric bands with a smooth function to obtain the wavelength dependence. Veiling is added first, assuming that all excess flux originates in regions close to the central object and is thus affected by scattering. Under these assumptions, we can fit the observed SED with $T_{\text{eff}} \sim 3000$ K, corresponding to a mass of $\sim 0.1 M_{\odot}$ at 1.0 Myr. In Fig. 2 we show spectra for three plausible scattering models (MRN2, 12, 15 in Kenyon et al. 1993), all with $T_{\text{eff}} = 3000$ K and veiling, as described above. Stronger veiling, as usually seen for Class I sources (Doppmann et al. 2005), would further reduce the photospheric contribution to the K-band flux and allow for deeper H_2O features, thus lower T_{eff} and mass.

Interpreting the NIR SED for IRAS04325C is challenging and subject to large uncertainties. We have shown that under reasonable assumptions the observational constraints are well-explained by veiled emission from a central object with $0.03\text{--}0.1 M_{\odot}$ seen through an edge-on disk. Higher masses cannot be strictly ruled out, but would require unusual scattering characteristics.

2.3. Spitzer photometry

IRAS04325 has been observed with Spitzer IRAC/MIPS as part of the Taurus Spitzer Legacy Project (PI: D. Padgett). The spatial resolution of MIPS is not sufficient to properly resolve the system; the combined fluxes for the source, as given in the

Taurus-1 source catalogue, are 1.9 Jy at $24\mu\text{m}$ and 4.7 ± 0.9 Jy at $70\mu\text{m}$. For comparison: The IRAS mid-infrared fluxes for this object are 2.1 Jy at $25\mu\text{m}$ and 12.86 Jy at $60\mu\text{m}$, again indicating that long-wavelength data with large apertures include significant extended background emission (see Sec. 2.1).

In the IRAC images, the object is clearly not point-like and shows two emission peaks coinciding with the positions of the two components, superimposed onto a bright nebosity. We carried out resolved photometry at $3\text{--}8\mu\text{m}$ by fitting the PSF in apertures with $3''.6$ radius centered on the peaks of the two components. We estimate the fluxes of the companion to be 4.1, 3.5, 2.6, 1.8 mJy at wavelengths 3.6, 4.5, 5.8, and $8.0\mu\text{m}$ (uncertainty $\pm 20\%$). Owing to the difficulties in disentangling the emission from the sources and from the underlying nebosity, the true Spitzer fluxes of IRAS04325C are likely to be significantly smaller. Comparing with the L-band flux published by Connelley et al. (2008) indicates that the background contamination may be as much as $\sim 70\%$. The fluxes of the primary source in the system are about 6, 7, 10, 11 times higher for IRAC channels 1–4, respectively.

3. MODELING THE SED OF IRAS04325C

We compiled the SED for IRAS04325C from our new observations and the literature. In the NIR, we aim to reproduce the K- and L-band fluxes from Connelley et al. (2008). The Spitzer fluxes are considered to be upper limits, as outlined in Sec. 2.3. In Fig. 3 we compare the observed SED with three model SEDs from a Monte Carlo radiation transfer code, which has been used successfully to model the SEDs of T Tauri stars (Wood et al. 2002) and brown dwarfs (Scholz et al. 2006). The models use NextGen model atmospheres for the photosphere (Allard et al. 2001) and include dust destruction close to the central object. Accretion rates are assumed to be negligible for the heating of the disk. For more details on the model ingredients, see Scholz et al. (2006). In all three models, we fix the disk radius at 30 AU, as given by Hartmann et al. (1999) based on the analysis of the HST images, the extinction at $A_V = 10$, and the parameters of the central object at values consistent with our spectroscopy ($T_{\text{eff}} = 2600$ K, $M = 0.07 M_{\odot}$). In addition, the model contains an infalling envelope with a bipolar cavity.

The models shown with solid and dashed line assume an inclination of $i = 80^\circ$ and two different grain size distributions: small ISM-type grains (solid line) and larger grains (dashed line), mimicking the effect of dust coagulation. In the latter case, the grain size distribution is a power law with an exponential decay for particles with sizes above $50\mu\text{m}$ and a formal maximum grain size of 1 mm, see Wood et al. (2002). Both models are able to provide a good match to the available datapoints. To fit the mm datapoint we need a total circumstellar mass of $2.2 \times 10^{-3} M_{\odot}$ for ISM grains and $4.6 \times 10^{-4} M_{\odot}$ for the larger grains. In the second case, the value for the disk/envelope mass is lower than the constraint given in Sec. 2.1 due to the higher dust opacity. Note that the two models are highly discrepant in their prediction for the fluxes at $5\text{--}20\mu\text{m}$ due to the different scattering albedo of the two grain types.

For illustration purposes, we also provide the SED for a

face-on geometry in dash-dotted lines. Clearly, the model is not in agreement with the observations. No combination of T_{eff} and A_V is able to fit both the observed fluxes and the near-infrared spectral slope, as discussed in Sec. 2.2.

In summary, the modeling clearly confirms the plausibility of the results obtained in earlier sections. The observed SED can be reproduced assuming that the central source is a very low mass star or brown dwarf, the inclination is high (i.e. the object is seen mostly in scattered light), and the circumstellar mass is negligible compared with the object mass. The models also demonstrate that more complete wavelength coverage is needed for further analysis of the properties of the system.

4. THE NATURE OF IRAS04325C

We present new observational constraints on the nature of the potential young brown dwarf IRAS04325C, a $8''$ companion to a well-known IRAS source discovered by Hartmann et al. (1999) in HST/NICMOS images. From our NIR spectrum for IRAS04325C, we estimate that the central source likely has a mass between 0.03 and 0.1 M_{\odot} . The available constraints on the infrared SED are inconsistent with a reddened photospheric spectrum, but they can be understood by assuming that the object is seen in scattered light. This is independent confirmation for the edge-on geometry of the disk, as seen in the HST images. IRAS04325C is only the second case of an edge-on system in the mass range $\lesssim 0.1 M_{\odot}$ that has been resolved with high-resolution imaging.

We detect the source with 1.3 mm interferometry at a flux level of 10 mJy, corresponding to a mass of 1–10 M_{Jup} in a localized disk/envelope with $R \lesssim 300$ AU. Since the accretion reservoir in a larger-scale envelope is probably insignificant, the central source is unlikely to gain more mass than 0.01 M_{\odot} due to further accretion. Thus, IRAS04325C will probably become either a very low mass star close to the substellar boundary or a brown dwarf.

The evolutionary stage of IRAS04325C is not well-determined based on the current data. The primary component of the system has been classified as a Class I source based on the mid-infrared spectral slope ($\alpha(2-25) = 0.79$, Duchêne et al. 2004) and the NIR colours (Lada & Adams 1992). It is also assumed to drive a CO

outflow (e.g. Hogerheijde et al. 1998), another characteristic for a protostellar source. The companion is clearly embedded in the same cloud core and likely physically bound to the primary, thus the two sources can be assumed to be coeval. This would make IRAS04325C the lowest mass Class I source known to date. The classification of the primary source, however, is partly based on unresolved data, including light from the companion and the surrounding nebulosity. Furthermore, the disk of the primary is probably seen close to edge-on ($i \sim 80^\circ$, Furlan et al. 2008), which would suppress the NIR flux and might lead to its misidentification as Class I source (see White et al. 2007). We estimate a total mass of a few Jupiter masses in a localised disk+envelope for the primary source, which seems to be too low for a Class I object (Andrews & Williams 2005). Thus, the Class I nature of the source is questionable.

The central source of IRAS04325C has probably significantly less mass than the primary component in the system. In all near/mid-infrared-bands, IRAS04325C is about an order of magnitude fainter than the primary source, indicating a mass ratio of ~ 0.15 . The luminosity of the primary has been estimated to be 0.7–0.9 L_{\odot} (Kenyon et al. 1993; Furlan et al. 2008), implying a mass of $\sim 0.7 M_{\odot}$. IRAS04325C also has a much smaller disk than the primary object, as seen in the HST images.

With its combined properties – very low mass central object, edge-on disk, wide companion to a more massive star – IRAS04325C is a prime target for follow-up studies and presents us with a unique opportunity to study the early evolutionary stages in a critical mass range.

This work is based on observations carried out with the IRAM Plateau de Bure Interferometer. IRAM is supported by INSU/CNRS (France), MPG (Germany) and IGN (Spain). We would like to thank the staff at IRAM, in particular Jan-Martin Winters and Vincent Pietu, for support with observations and data reduction. The help provided by John Rayner during the SpeX observations is appreciated. Parts of this study are based on archival data obtained with the Spitzer Space Telescope, which is operated by the Jet Propulsion Laboratory, California Institute of Technology under a contract with NASA.

REFERENCES

- Allard, F., Hauschildt, P. H., Alexander, D. R., Tamanai, A., & Schweitzer, A. 2001, *ApJ*, 556, 357
 Andrews, S. M., & Williams, J. P. 2005, *ApJ*, 631, 1134
 Baraffe, I., Chabrier, G., Allard, F., & Hauschildt, P. H. 1998, *A&A*, 337, 403
 Connelley, M. S., Reipurth, B., & Tokunaga, A. T. 2008, *AJ*, 135, 2496
 Cushing, M. C., Vacca, W. D., & Rayner, J. T. 2004, *PASP*, 116, 362
 Doppmann, G. W., Greene, T. P., Covey, K. R., & Lada, C. J. 2005, *AJ*, 130, 1145
 Duchêne, G., Bouvier, J., Bontemps, S., André, P., & Motte, F. 2004, *A&A*, 427, 651
 Folha, D. F. M., & Emerson, J. P. 1999, *A&A*, 352, 517
 Furlan, E., et al. 2008, *ApJS*, 176, 184
 Greene, T. P., & Lada, C. J. 1996, *AJ*, 112, 2184
 Guilloteau, S., et al. 1992, *A&A*, 262, 624
 Hartmann, L., Calvet, N., Allen, L., Chen, H., & Jayawardhana, R. 1999, *AJ*, 118, 1784
 Hogerheijde, M. R., van Dishoeck, E. F., Blake, G. A., & van Langevelde, H. J. 1998, *ApJ*, 502, 315
 Hogerheijde, M. R., & Sandell, G. 2000, *ApJ*, 534, 880
 Kenyon, S. J., Whitney, B. A., Gomez, M., & Hartmann, L. 1993, *ApJ*, 414, 773
 Kenyon, S. J., & Hartmann, L. 1995, *ApJS*, 101, 117
 Klein, R., Apai, D., Pascucci, I., Henning, T., & Waters, L. B. F. M. 2003, *ApJ*, 593, L57
 Lada, C. J., & Adams, F. C. 1992, *ApJ*, 393, 278
 Loinard, L., Torres, R. M., Mioduszewski, A. J., Rodríguez, L. F., González-Lópezlira, R. A., Lachaume, R., Vázquez, V., & González, E. 2007, *ApJ*, 671, 546
 Luhman, K. L., Adame, L., D'Alessio, P., Calvet, N., McLeod, K. K., Bohac, C. J., Forrest, W. J., Hartmann, L., Sargent, B., & Watson, D. M. 2007a, *ApJ*, 666, 1219
 Luhman, K. L., Joergens, V., Lada, C., Muzerolle, J., Pascucci, I., & White, R. 2007b, in *Protostars and Planets V*, ed. B. Reipurth, D. Jewitt, & K. Keil, 443–457
 Mathis, J. S. 1990, *ARA&A*, 28, 37
 Motte, F., & André, P. 2001, *A&A*, 365, 440

- Natta, A., Testi, L., Calvet, N., Henning, T., Waters, R., & Wilner, D. 2007, in *Protostars and Planets V*, ed. B. Reipurth, D. Jewitt, & K. Keil, 767–781
- Ohashi, N., Hayashi, M., Kawabe, R., & Ishiguro, M. 1996, *ApJ*, 466, 317
- Rayner, J. T., Toomey, D. W., Onaka, P. M., Denault, A. J., Stahlberger, W. E., Vacca, W. D., Cushing, M. C., & Wang, S. 2003, *PASP*, 115, 362
- Scholz, A., Jayawardhana, R., & Wood, K. 2006, *ApJ*, 645, 1498
- White, R. J., Greene, T. P., Doppmann, G. W., Covey, K. R., & Hillenbrand, L. A. 2007, in *Protostars and Planets V*, ed. B. Reipurth, D. Jewitt, & K. Keil, 117–132
- Whitworth, A., Bate, M. R., Nordlund, Å., Reipurth, B., & Zinnecker, H. 2007, in *Protostars and Planets V*, ed. B. Reipurth, D. Jewitt, & K. Keil, 459–476
- Wood, K., Wolff, M. J., Bjorkman, J. E., & Whitney, B. 2002, *ApJ*, 564, 887